J. Membrane Biol. 105, 45–53 (1988)

The Journal of
Membrane Biology

Impermeant Potential-Sensitive Oxonol Dyes: II. The Dependence of the Absorption Signal on the Length of Alkyl Substituents Attached to the Dye

P. Nyirjesy†, E.B. George†, R.K. Gupta†, M. Basson†, P.R. Pratap‡, J.C. Freedman‡, K. Raman†, and A.S. Waggoner†§

§Department of Biological Sciences, Carnegie-Mellon University, Pittsburgh, Pennsylvania 15213, †Department of Chemistry, Amherst College, Amherst, Massachusetts 01002, and ‡Department of Physiology, SUNY Health Sciences Center, Syracuse, New York 13210

Summary. We have measured the potential-dependent light absorption changes of 43 impermeant oxonol dyes with an oxidized cholesterol bilayer lipid membrane system. The size of the signal is strongly dependent on the chain length of alkyl groups attached to the chromophore. Dye molecules with intermediate chain lengths give the largest signals. To better understand the dependence of the absorbance signal on alkyl chain length, a simple equilibrium thermodynamic analysis has been derived. The analysis uses the free energy of dye binding to the membrane and the "on-off" model (E.B. George et al., *J. Membrane Biol.*, **103**:245–253, 1988*a*) for the potential-sensing mechanism. In this model, a population of dye molecules in nonpolar membrane binding sites is in a potential-dependent equilibrium with a second population of dye that resides in an unstirred layer adjacent to the membrane. Dye in the unstirred layer is in a separate equilibrium with dye in the bulk bathing solution. The equilibrium binding theory predicts a "sigmoidally shaped" increase in signal with increasing alkyl chain length, even for very nonpolar dyes. We suggest that aggregation of the more hydrophobic dyes in the membrane bathing solution may be responsible for their low signals, which are not predicted by the theory.

Key Words potential-dependent dye · oxonol dye · membrane · lipid bilayer · dye binding · mechanism

Introduction

Potential-sensitive dyes frequently show signals that depend on the amount of hydrocarbon attached to the dye structure. One example includes the cationic cyanine dyes, which give *slow* (seconds to minutes) fluorescence changes in experiments with cell suspensions (Sims et al., 1974). These fluorescence changes result from potential-dependent redistribution of dye molecules across the membranes of the cells. Sims et al. (1974) observed that the largest fluorescence changes generally occur with cyanine analogs that possessed a pair of hydrocarbon chains of intermediate length. These dyes also responded most quickly to sudden potential changes. The signals from analogs with shorter or longer chains were generally much smaller and slower.

The membrane-permeant cyanine dyes and membrane-permeant anionic oxonol dyes are capable of giving *rapid* as well as slow absorption and fluorescence changes with excitable cells and lipid bilayers (Waggoner, Wang & Tolles, 1977). A rapid response (msec) to quick potential changes occurs as the probe molecules move between a hydrocarbon environment of the membrane and a more polar region that is probably in the water near the membrane but may be on the surface of the membrane. A slower response occurs as the dye molecules redistribute across the membrane during a long membrane potential change. The kinetics and magnitudes of both the slow and the rapid responses depend on the hydrocarbon content of the dye.

Another type of potential-sensitive dye is represented by Merocyanine 540. It is a membrane *impermeant* probe and therefore functions by a mechanism different from the permeant cyanine and oxonol dyes (Wolf & Waggoner, 1986). Nevertheless, the signal size of Merocyanine 540 changes when hydrocarbon groups attached to the chromophore are lengthened or shortened. Merocyanine 540 analogs with varying numbers (N) of CH_2 groups bound to the chromophore were synthesized

* *Present addresses:* EBG, Department of Neurology, Johns Hopkins Medical School, Baltimore, MD 21205; PN, Obstetrics Department, Thomas Jefferson University Hospital, Philadelphia, PA 19107; RKG, Coulter Immunology, Inc., 440 20th Street, Hialeah, FL 33010; MB, Department of Biology, MIT, Cambridge, MA 02139; KR, Warner Lambert, Inc., 175 Tabor Rd., Morris Plains, NJ 07950; ASW, Carnegie-Mellon University, 4400 5th Avenue, Pittsburgh, PA 15213.

and tested with the squid giant axon (Cohen et al., 1974). When butyl groups ($N = 4$) were attached to the barbituric acid nucleus of the chromophore the signal was large but analogs with longer or shorter aliphatic chains had smaller signals. The dependence of signal on N was identical for the squid experiments (Waggoner, 1976) and for oxidized cholesterol bilayer lipid membrane studies (Wolf & Waggoner, 1986). The latter authors went on to develop a thermodynamic model for the dependence of signal on N. The present work extends the model so that it can be applied to the impermeant oxonol probes.

The impermeant oxonols are another important class of potential-sensitive dyes that show a strong dependence of absorption and fluorescence signals on the hydrocarbon substituents attached to the chromophore structure (Gupta et al., 1981). Oxidized cholesterol membranes, while unphysiological and poorly defined, offered two advantages for this study. First, the membranes are relatively stable in the presence of a large number of different dye analogs. Second, the spherical configuration of the oxidized cholesterol membrane developed by Dragsten and Webb (1978) provided an excellent geometry for the polarization studies of the first paper in this series (George et al., 1988*a*). In the present study, we have measured the potential-dependent absorption change ΔA of 43 analogs of WW781 associated with oxidized cholesterol bilayer lipid membranes. In this model system, just as was observed with squid axons, ΔA depends strongly on the number of CH_2 group equivalents attached to the chromophore. The signals are largest for analogs with intermediate amounts of hydrocarbon. To gain insights into the mechanism of the dependence of ΔA on N, we have extended the thermodynamic treatment developed by Wolf and Waggoner (1986) for Merocyanine 540 analogs to the impermeant oxonols. The analysis relates ΔA to various dye-membrane binding constants which in turn are dependent on N.

Materials and Methods

The pyrazolone-barbituric acid and pyrazolone-thiobarbituric acid dyes were synthesized according to the procedure of Gupta et al., 1981. The oxidized cholesterol bilayer lipid membrane system for detecting optical signals is described in the previous paper (George et al. (1988*a*). Changes (ΔI) in the intensity of quasimonochromatic light passing through the bottom of the oxidized cholesterol hemispherical bilayer membrane (apparatus details in George et al., 1988*a*) were measured during a train of 5-msec voltage steps that alternated between −50 and +50 mV. The light transmission changes were converted to absorbance changes (ΔA) with the relationship $\Delta A = -\Delta I/2.3I$ (Waggoner & Grinvald, 1977). The ΔA quoted in Fig. 2 and in the Table were measured at the wavelength where the maximum signal was obtained (630 nm for the barbituric acid derivatives and 660 nm for the thiobarbituric acid analogs). Absorption spectra were obtained as described by George et al. (1988*a*).

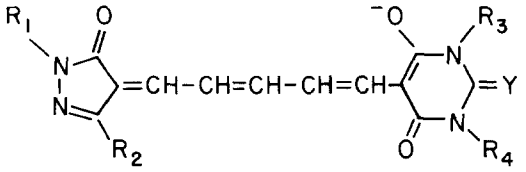

Fig. 1. General structure of the pyrazolone-barbituric acid (Y = O) and pyrazolone-thiobarbituric acid (Y = S) dyes. The R groups are indicated in the Table

Results

The general structure of the oxazalone-barbituric acid and pyrazolone-thiobarbituric acid dyes is shown in Fig. 1. Attached to the chromophore are a number of substituents. The R_1 group for all of the dyes studied in this work is either an alkylsulfonate or an arylsulfonate (*see* Table). Just as it does with Merocyanine 540, the localized negative charge of the sulfonate acts as an anchor to keep the chromophore from penetrating too deeply into the membrane and to prevent it from crossing to the opposite side. Oxonols without this group are usually membrane permeant (Sims et al., 1974; Waggoner et al., 1977; Bashford et al., 1979). The R_2, R_3, and R_4 groups are hydrocarbon substituents that play a major role in determining the strength of binding of the chromophore to the membrane.

The relative hydrocarbon content of the analogs can be quantified as follows. When the hydrocarbon substituent is an alkyl chain, the number of carbons N in the chain are designated as CH_2 equivalents. Thus, a butyl-group contributes a value of 4 to the number of CH_2 equivalents on the chromophore. For more complicated groups, like esters and aromatic groups, an estimate of the number of CH_2 equivalents is based on data on the free energy of transfer of the group from water to a hydrocarbon solvent as compared to the free energy of transfer for a CH_2 group (Diamond & Katz, 1974; Tanford, 1980). These estimates are listed in the Table. The total number of CH_2 equivalents for each dye is listed as an N value in the Table. No distinction between alkyl groups that are attached to the barbituric acid *vs.* those on the pyrazolone nucleus has been made.

The impermeant oxonol analogs were each tested in the oxidized cholesterol bilayer lipid membrane system to determine how the voltage-dependent absorbance signal strength ΔA depends on N.

Table. Absorbance signals (ΔA) for impermant oxonol analogs[a]

Dye name	Y	R_1	R_2	R_3	R_4	N	$\Delta A \times 10^6$
WW781	O	A[b]	1	4	4	9	9
WW802	O	A	1	5	5	11	20
RGA460	O	A	2	3	3	8	7
RGA459	O	A	2	4	4	10	12
RGA461	O	A	2	5	5	12	35
RGA592	O	A	2	6	6	14	43
RGA570A	O	A	3	5	0	8	5
RGA570	O	A	3	5	5	13	21
RGA485	O	A	5	4	4	14	16
RGA495	O	A	13	4	4	21	5
RGA480	O	A	17	4	4	25	2
RGA451	O	A	M	3	3	10	11
RGA445	O	A	M	4	4	12	15
RGA450	O	A	M	5	5	14	16
RGA448	O	A	N	4	4	11	18
RGA512	O	A	P	3	3	8	10
RGA452	O	A	P	4	4	10	16
RGA514	O	A	P	5	5	12	23
RGA497	O	A	Q	4	4	10	7
RGA500	O	A	R	4	4	11	14
DR696	O	B	1	4	4	9	7
RGA422	O	C	M	4	4	12	19
RGA590	O	C	2	5	5	12	37
RGA588	O	C	M	5	5	14	37
RGA526	O	H	1	4	4	10	7
RGA456	O	G	1	4	4	10	10
RGA528	O	I	1	4	4	12	13
RGA585	O	I	1	3	3	10	5
RGA589	O	I	1	5	5	14	16
RGA529	O	J	1	4	4	15	19
RGA483	O	K	3	4	4	10	7
RGA481	O	L	1	4	4	9	3
RGA482	O	L	3	4	4	11	24
RGA316	S	A	1	2	2	5	3
RGA338b	S	A	1	3	3	7	4
RGA33a	S	A	1	4	4	9	20
RGA339	S	A	1	5	5	11	27
RGA17	S	A	1	6	6	13	17
RGA28a	S	A	1	8	8	17	17
RGA20	S	A	1	18	4	23	4
RGA572	S	A	2	5	5	12	12
RGA444	S	B	1	2	2	5	4
RGA317a	S	D	1	2	2	5	1

[a] Under column Y, an O stands for a barbituric acid analog (*see* Fig. 1) and an S represents a thiobarituric acid analog. Numerical values in columns headed by R_1, R_2, R_3, and R_4 correspond to the number of CH_2 groups in the respective positions on the structure in Fig. 1. Letter symbols in the R-group columns correspond to substituents listed below. Values listed under N are the sum of the values for the 4 R groups.

[b] Designations:

A = 4-sulfophenyl	$N = 0$
B = 3-sulfophenyl	$N = 0$
C = 2-sulfophenyl	$N = 0$
D = 4-carboxyphenyl	$N = 0$
G = 3,6-dichloro-4-sulfophenyl	$N = 1$
H = 1-methyl-4-sulfophenyl	$N = 1$
I = 2-(5,7-disulfonaphthyl)	$N = 3$
J = 4-(7-sulfo-6-methyl-2-benzothiazolyl)-phenyl	$N = 6$
K = 3-sulfopropyl	$N = -1$
L = 3-sulfobutyl	$N = 0$
M = phenyl	$N = 4$
N = $-CH_2CO_2Et$	$N = 3$
P = $-CO_2Et$	$N = 2$
Q = $-CH_2CO_2Me$	$N = 2$
R = $-C(CH_3)_3$	$N = 3$

The apparatus for making these determinations is described in the previous paper (George et al., 1988*a*). The values of ΔA for each analog are listed in the Table and ΔA *vs.* N is plotted in Fig. 2(*A*). When experiments were repeated, signals were usually within 20% of each other, but occasionally they varied by as much as 50% (*see* a more detailed discussion analysis of sources of experimental error in the Materials and Methods section of George et al., 1988*a*). Many of the values in the Table are for single experiments and some are averaged values for repeated experiments.

Figure 2(*A*) illustrates that the maximum signals are found for analogs with N in the vicinity of 12–14. Dyes with much more or much less attached hydrocarbon have smaller signals.

Absorption spectra were obtained for each of the analogs in the Table after they were dissolved in methanol and in 100 mM KCl, the solution in which the membranes were bathed. The more hydrophobic dyes ($N > 15$) at 6 μM in 100 mM KCl showed blue-shifted absorption peaks compared with the less hydrophobic analogs ($N = 5 - 10$). An example of this effect is shown in Fig. 3. Blue shifts are indicative of the formation of dimers and low-order aggregates of dye (Sims et al., 1974). Each of the analogs that gave spectroscopic evidence of moderate to strong aggregate formation is indicated separately in Fig. 2(*A*). It is clear that the analogs with $N > 15$ have reduced optical signals and form aggregates in the bathing solution.

Three of the analogs bear an extra negative charge that raises the total charge on the probe from 2 to 3. The three analogs (RG528, RG585, and RG589 indicated separately in Fig. 2*A*) each give a signal that is somewhat lower than that obtained with other dyes of equivalent N. Generally speaking, however, there were no obvious differences between the barbituric acid and thiobarbituric acid analogs with equivalent N or between analogs in which equivalent hydrocarbon groups were located on different regions of the chromophore.

Analysis and Discussion

Below we will derive an approximate equation for the dependence of the absorption signal on N. We will use a simple thermodynamic analysis of the

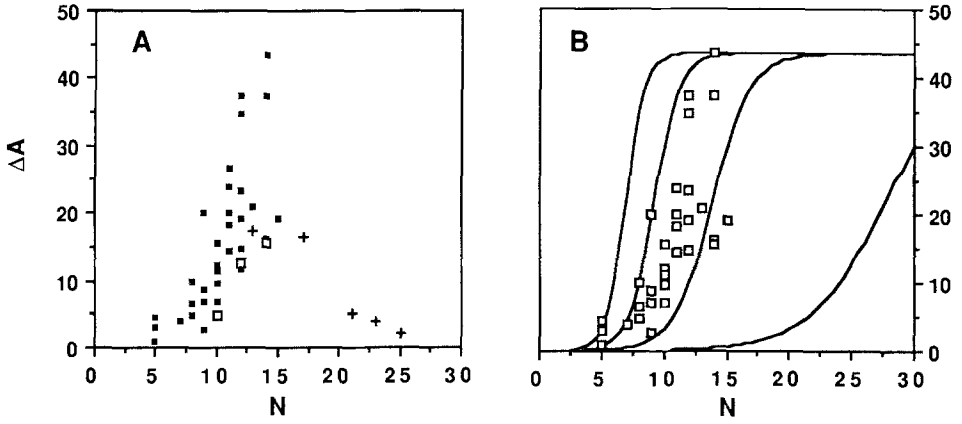

Fig. 2. (*A*) Absorption signals *vs.* hydrocarbon content of the impermeant oxonol dyes in the Table. Open squares: analogs bearing three negative charges (RG528, RG585, RG589). Crosses: analogs that showed spectral evidence of aggregate formation in 100 mM KCl. Filled squares: remaining data from the Table. (*B*) Absorption signals *vs.* hydrocarbon content. Theoretical curves: generated from Eq. (7). The ΔG_{CH_2} values (kcal/mol) for the curves are: −0.2, −0.4, −0.6, −0.8, respectively, starting from the right. Other constants used: $\beta = 0.05$, $\Delta V = 100$ mV. Maximum height of curves normalized to signal size of dye GR592. Open squares: Experimental data from the Table. Trivalent and aggregating dyes excluded (*see* Fig. 2*A*)

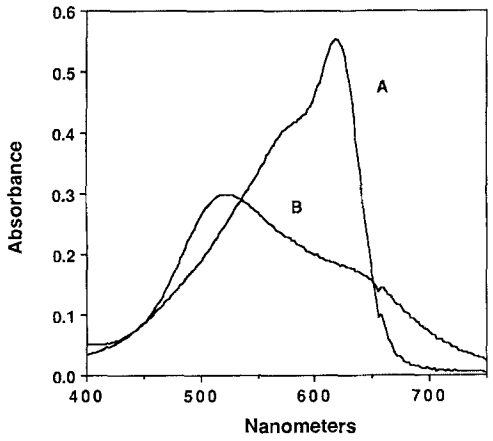

Fig. 3. Absorption spectra of a less hydrophobic analog (RG317a, $N = 5$) and a closely related (except for hydrocarbon content) analog that is more hydrophobic (RG28a, $N = 17$). Both probes are at a concentration of 6 μM in 100 mM KCl. Spectra were obtained 5 min after dilution of dye from a concentrated mentanol stock solution

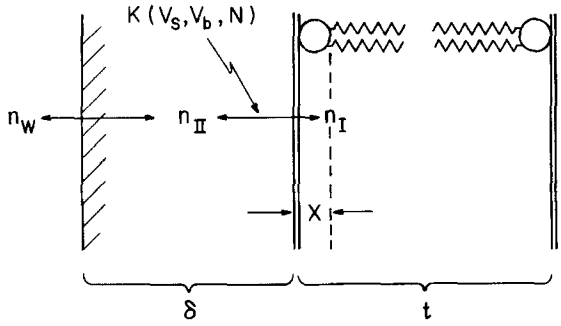

Fig. 4. Schematic diagram of "on-off" model. The quantities of dye in the three populations are indicated by n_I, n_{II}, and n_w. The membrane-bound population sits at a depth x in a membrane of thickness t. Population II resides in a ∂-cm thick aqueous region adjacent to the membrane. The concentration of dye in the solution bathing the membrane is n_w. The equilibrium constant for distribution of dye between sites I and II is a function of the step size of the voltage pulse train (V_s), the bias voltage across the membrane (V_b), and the hydrocarbon content of the dye (N)

"on-off" model for the impermeant oxonol mechanism.

Quantitative Definition of the "On-Off" Model

Paper I of this series (George et al., 1988*a*) provides spectral data that supports an "on-off" mechanism for the potential sensitivity of the impermeant oxonol, RGA 461, which is one of the most sensitive of the pyrazolone-barbituric acid dyes (Table). In the "on-off" model, which is shown in Fig. 4, the dye residues in three sites. Site I is buried at a depth x in a nonpolar region of the membrane which has a thickness t. Site I contains n_I moles of dye per cm^2.

Site II is in an unstirred aqueous region of thickness ∂ adjacent to the surface of the membrane. Site II is occupied by n_{II} moles of dye per cm^2. The relative populations in sites I and II are membrane potential dependent. Positive potential pulses drive the negatively charged chromophore part of the dye into the hydrocarbon region of the membrane with the long axis of the chromophore oriented more or less perpendicular to the surface of the membrane (George et al., 1988*a*). The sulfonate group on the

dye remains at the surface and prevents the probe from crossing to the opposite side of the membrane. The thickness of region II is determined by the distance that dye molecules moving to and from the membrane can diffuse during the 5 msec membrane potential steps used in the experiment. By using a diffusion coefficient for the dye of 4×10^{-6} cm^2 sec^{-1} (Smith et al., 1980), the mean square distance of diffusion is about 10^{-4} cm. We use this value for ∂.

The aqueous bathing medium provides the third population n_w, which has concentration units, moles/cm^3. The dye in region II and in the bathing medium are in equilibrium so the average concentration of dye in region II (independent of the rapid voltage pulses) is given by $n_{II}^{avg}/\partial = n_w$. In this model we have not included the possibility that dye might move from the hydrocarbon binding site (I) to a membrane surface binding site instead of (or as well as) moving from the hydrocarbon site directly into the aqueous ∂-region. Spectral evidence collected by George et al. (1988*a*) weighs against this possibility.

Theoretical Description of the Dependence of ΔA on N

ΔA describes the potential-dependent change in dye absorbance that occurs when a train of voltage steps is applied to a membrane in a solution containing dye. More specifically, $\Delta A = 1000\ \Delta E \Delta n$, where ΔE is the change in the extinction coefficient of the dye as it moves between the potential-dependent sites and Δn is the number of moles of dye per square centimeter moving between the two sites (Waggoner & Grinvald, 1977). We assume that ΔE is the same for the 43 dyes in this study and therefore we will now focus our concern only on how ΔA, which is proportional to Δn, varies with N. The derivation below is more general and seeks to express the dependence of Δn on the membrane potential as well as on N.

Consider first the factors that control the ratio of the number of dye molecules in sites I and II. The impermeant oxonol probes are doubly charged and hydrophobic. Thus the free energy difference for the probe in sites I and II will involve an electrical and a chemical component. Following the lead of a number of investigators (Ketterer, Neumcke & Läuger, 1971; Andersen et al., 1978; Flwelling & Hubbell, 1986), who have analyzed the similar interactions of hydrophobic ions, like tetraphenylphosphonium (TPP^+) and tetraphenylborate (TPB^-), with membranes, we can describe the distribution of the impermeant oxonols with Eq. (1), where R is the gas constant, T is the Kelvin temperature:

$$\frac{n_I}{n_{II}} = e^{-(\Delta G(N=0)+N\cdot\Delta G_{CH_2}+\Delta G(V))/RT}. \quad (1)$$

In this equation, $\Delta G(N = 0)$ is the free energy change for the transfer of the probe without alkyl substituents from the aqueous environment in region II to the nonpolar environment of site I in the absence of any transmembrane electrical potential. $\Delta G(N = 0)$ is largely due to the burial of the hydrophobic chromophore in the membrane, but it also includes the interactions of the charges on the probe with the membrane (Anderson et al., 1978; Krasne, 1980; Flewelling & Hubbell, 1986). In the terminology of Honig, Hubbell and Flewelling (1986), $\Delta G(N = 0)$ is the sum of the Born energy, the image energy, the dipole energy, and the neutral energy.

Although oxidized cholesterol membranes are neutral, the binding of the doubly negatively charged oxonol molecules at high surface densities adds a significant charge to the membrane that will limit the binding of additional molecules of dye to the membrane. For example, the saturation of TPB^- and TPP^+ binding to membranes has been observed experimentally and has been attributed to repulsions between bound ions (Ketterer et al., 1971; Andersen et al., 1978). Krasne (1980) has quantified the magnitude of bilayer surface potentials (and boundary potentials) generated by the binding of cyanine and oxonol dyes. She found that, up to a point, the analogs with longer alkyl chains produced larger surface potentials. Surface potentials up to +60 mV were observed with 100 mM KCl solutions containing 1 to 10 μM cyanine dye. For the impermeant oxonols, we expect the sulfonate group at the surface of the membrane to contribute to the surface potential. The surface potential is a function of the ionic strength of the bathing solution as well as of n_I (Davies, 1958; McLaughlin, 1977; Krasne, 1980). On the other hand, the charged chromophore part of the dye, which lies beneath the membrane surface, will contribute mainly to the boundary potential, which is less affected by ionic strength.

At this point a major approximation is made in order to simplify steps in the derivation that will follow. Surface potential and boundary potential energies, which increase as N increases, and which limit the amount of dye that can bind to the membrane, will be assumed to remain negligible for all the analogs. This approximation may not be reasonable for the impermeant oxonol dyes that have a high affinity for the membrane (e.g. $N > 15$). It is even possible that dyes with intermediate alkyl chain lengths may nearly saturate the membrane.

The second term in the brackets of Eq. (1) gives the free energy change for transfer of the alkyl chains of the dye from the bathing solution to the

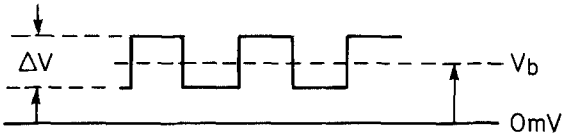

Fig. 5. Membrane voltage pulse train used to obtain optical signals. Step potential changes (ΔV) and offset, or bias, potential (V_b) are indicated

membrane. ΔG_{CH_2} is the free energy of transfer per CH_2 group. Other studies of the binding of alkyl compounds of different chain lengths to surfaces (Davies, 1958) and to membranes (Diamond & Katz, 1974) indicate that the free energy of transfer depends linearly on the number of CH_2 groups. Furthermore, they found that ΔG_{CH_2} is in the range of -0.5 to -0.8 kcal/mol, depending on the nature of the membrane binding site.

The third term in Eq. (1), $\Delta G(V)$, is the part of the electrical free energy change for the movement of probe from II to I that can be attributed only to the transmembrane electrical potential. $\Delta G(V)$ has the form $-ZF\beta(V_s + V_b)$, where V_b is the offset, or bias, potential, as defined in Fig. 5, and V_s is the voltage step potential superimposed on V_b. For a train of square voltage pulses of magnitude ΔV, V_s has the values $\pm\Delta V/2$. Since the charged region of the oxonol chromophore only penetrates a fraction of the way through the membrane, the membrane potential sensed by the probe is some fraction β of the sum of the transmembrane potential.

It is useful to express the exponentials of Eq. (1) that depend on N and V_b as equilibrium constants. So, let $K(N) = \exp(-\Delta G(N = 0)/RT - N^*\Delta G_{CH_2}/RT)$ and $K(V_b) = \exp(ZF\beta V_b/RT)$. Now the population ratios during positive and negative steps can be written as follows, where $\gamma = ZF/RT$:

$$\frac{n_I^+}{n_{II}^+} = K(N)K(V_b)e^{-\gamma\beta\Delta V/2} \tag{2a}$$

$$\frac{n_I^-}{n_{II}^-} = K(N)K(V_b)e^{+\gamma\beta\Delta V/2} \tag{2b}$$

The change in the amount of dye in each population during a train of voltage pulses is given by Eq. (3):

$$\Delta n = n_I^+ - n_I^- = n_{II}^- - n_{II}^+. \tag{3}$$

Before a final expression for Δn can eventually be obtained, an equation for the total amount of dye n_T in populations I and II must be obtained. The value of n_T given in Eq. (4) is independent of the potential steps, which drive a wave of dye molecules back and forth between the two sites.

$$n_T = n_I^+ + n_{II}^+ = n_I^- + n_{II}^- = n_I^{avg} + n_{II}^{avg}. \tag{4}$$

The average distribution of dye between sites I and II is independent of V_s and is determined only by the binding constants, $K(N)$ and $K(V_b)$. Thus $n_I^{avg}/n_{II}^{avg} = K(N)K(V_b)$. When this expression is combined with Eq. (4), we find that n_T equals $n_{II}^{avg}[1 + K(N)K(V_b)]$. Since n_{II}^{avg} is equal to the concentration of dye in the medium times the thickness of region II, a simple expression for n_T can be obtained.

$$n_T = n_W\partial(1 + K(N)K(V_b)). \tag{5}$$

By placing Eqs. (2a) and (2b) into the appropriate equalities in Eq. (4), it is possible to derive expressions for the amount of membrane-bound dye during positive and negative potential steps:

$$n_I^+ = \frac{n_T K(N)K(V_b)e^{-\gamma\beta\Delta V/2}}{1 + K(N)K(V_b)e^{-\gamma\beta\Delta V/2}} \tag{6a}$$

$$n_I^- = \frac{n_T K(N)K(V_b)e^{+\gamma\beta\Delta V/2}}{1 + K(N)K(V_b)e^{+\gamma\beta\Delta V/2}}. \tag{6b}$$

Insertion of Eqs. (6a) and (6b) into Eq. (3), with the necessary rearrangements, followed by substitution of the expression for n_T given in Eq. (4), leads to the desired equation for the potential-dependent population shift.

$$\Delta A \propto \Delta n = \frac{n_W\partial p(1 + p)(q - r)}{(1 + pq)(1 + pr)} \tag{7}$$

where:

$$p = K(N)K(V_b)$$
$$q = e^{-\gamma\beta\Delta V/2}$$
$$r = e^{+\gamma\beta\Delta V/2}.$$

Equation (7) is the most general equation for the absorbance signal of a membrane-impermeant dye responding by the "on-off" mechanism with the restriction that the surface potential and other factors that lead to saturation binding are ignored. This equation will also be used for the analysis of the voltage dependence of absorbance signals in the third paper of this series (George et al., 1988*b*).

In order to use Eq. (7) to generate a series of curves (shown below in Fig. 2*B*) describing the theoretical dependence of ΔA on N in the absence of a bias potential ($V_b = 0$ mV), we let $K(V_b) = 1$ and insert the dependence of $K(N)$ on the free energy change for dye binding to the membrane per additional CH_2 group given by Eq. (8)

$$K(N) = K(N = 0)e^{-N\cdot\Delta G_{CH_2}/RT}. \tag{8}$$

In Eq. (8), the equilibrium constant for the probe in the absence of alkyl substituents, $K(N = 0)$ equals $\exp(\Delta G(N = 0)/RT)$ [*see* Eq. (1)] and is assumed to have the same value for all of the dyes used in this study.

Analysis of the ΔA *vs.* N Data

Figure 2*B* includes computer generated curves from Eq. (7) that illustrate the theoretical dependence of ΔA on N for values of ΔG_{CH_2} ranging from -0.2 to -0.8 kcal/mol. In generating these curves, ΔV was set to 100 mV (experimental condition used), and 0.05 was used for β (George et al., 1988*b*). The resulting curves were relatively insensitive to changes in ΔV within a factor of 10. Curves were normalized to the maximum optical signal value that was obtained with dye RG592.

The horizontal location of the families of curves on the graph is sensitive to $K(N = 0)$. Values of $K(N = 0)$ from 10^{-3} to 10^{-4} (the value used to generate the curves shown in Fig. 2) place these families of curves upon the experimental data. For $K(N = 0) = 10^{-4}$, curves with ΔG_{CH_2} values between -0.4 and -0.6 kcal/mol bracket most data points for N less than 16, whereas a range of -0.3 to -0.5 kcal/mol is better when $K(N = 0)$ is 10^{-3}. When $K(N = 0)$ is smaller than 10^{-4} the curves are too steep and when $K(N = 0)$ is larger than 10^{-2} they are too shallow. The ΔG_{CH_2} values that give the best fit (-0.3 to -0.6 kcal/mol) are characteristic of transfer of CH_2 groups into solvents of moderately low polarity.

Discussion

The data for ΔA *vs.* N illustrate the strong dependence of optical signal on the number of nonpolar residues attached to the potential-sensitive probe. More hydrophobic dyes partition strongly into the membrane, and up to a point, give larger signals. The polarity of the dye analogs used in this study is determined mainly by the number of CH_2 groups attached to the chromophore. Each CH_2 group contributes a free energy change in the range of -0.3 to -0.6 kcal/mol as the probe moves from the bathing medium to the membrane-binding site. Thus the analysis suggests that the CH_2 groups attached to the dyes interact with a region of intermediate polarity in the membrane.

It would be interesting to extend the analysis to subsets of dyes in which the alkyl groups located near the sulfonate group as opposed to near the barbituric acid or thiobarbituric acid rings are varied. Light polarization studies (George et al., 1988*a*) indicate that membrane-bound probe is probably oriented with the sulfonate end of the probe near the surface and the (thio)barbituric acid end imbedded in the hydrocarbon region of the membrane. Thus analogs with alkyl substitutions on the (thio)barbituric acid nucleus may show larger values of ΔG_{CH_2} because their alkyl chains extend into a more nonpolar region of the membrane. For these comparisons, additional analogs would have to be synthesized and the experiments would have to be repeated more times to obtain better statistics.

The theoretical analysis we have used produces a "sigmoid-shaped" dependence of ΔA on N, whereas the experimental signal decreases at large N. The dependence of ΔA on N predicted by the theory seems reasonable. One might expect the signal to monotonically increase with N as more dye binds to the membrane where it can sense the membrane potential change. The signal eventually saturates at high N because the voltage steps cannot provide sufficient driving force to displace the more tightly bound dye molecules from the membrane.

We shall now turn our attention to possible explanations for the loss of experimental signal at high N, which is not predicted by the theory.

Possibility 1. The signal may decrease at large N because the membrane binding sites become saturated with probe. Saturation of lipid bilayers with monovalent hydrophobic molecules occurs in the vicinity of 0.7 to 30 picomoles per sq cm (George et al., 1988*b*, Table 2). George et al. (1988*a*) found that the absorption signal of RGA461 ($N = 12$) saturates with approximately 6–12 μM dye in the bathing medium. Probes with higher membrane association constants (large N) would be expected to saturate the membrane even when used at lower concentrations than the one used in this study (6 μM). However, saturation alone would not reduce the signal size as long as the negative steps of the pulse train can still drive a large amount of dye off the saturated membrane. Positive pulses should easily drive the return of the dye to the vacated sites. Thus, one might expect the signal to plateau when saturation occurs, but it is not obvious that saturation of membrane binding sites at high N explains the loss of signal for these dyes. On the other hand, if saturation occurs, and at the same time the amount of dye that can be displaced from the membrane decreases because dye molecules with large N are tightly bound, one would expect a loss of signal when N is large.

Possibility 2. This consideration is a kinetic one. Dye molecules with high affinities for hydrocarbon regions of the membrane may have small rate constants for movement out of site I. As a result, a short potential pulse would be over before much probe could move to the aqueous compartment. Potential steps in the reverse direction would be equally ineffective since no spaces would have been opened in site I for the return of the dye. The

experiments we have done in this study do not shed any light on possible kinetic effects partly because the signals from dyes with large N were too small to analyze their time responses.

Possibility 3. We have obtained spectroscopic evidence that the more hydrophobic dyes ($N > 15$) form aggregates in the 100 mM KCl solution that bathes the membranes. It is possible that the formation of micelles, aggregates, or microcrystals in the bathing solution reduces the absorbance signal. With each of these aggregated species there is a reduction in the concentration in region II of monomeric dye molecules that can participate in the "on-off" mechanism. Furthermore, it is likely that the rate of movement of probe molecules from aggregate particles to the oxidized cholesterol membrane is slow compared with the rate at which monomers move between the aqueous phase and the membrane. Thus kinetic restraints would limit the size of the absorption signal.

The results of this study illustrate the sensitivity of potential-dependent absorption changes to the structure of the probe molecules. Signals from impermeant "on-off" dyes can be enhanced by increasing the amount of probe bound to the membrane. To a point this can be done by raising the concentration of dye in the bathing medium and by increasing the membrane association constant of the dye by attaching hydrocarbon residues to the dye. However, absorbance signals eventually saturate at high dye concentrations (George et al., 1988*a*). And when dye molecules become too hydrophobic they form aggregates in the bathing solution and the signal is reduced.

We have evidence (Fig. 2*A*) that addition of more charge to the polar part of the impermeant oxonols reduces their signals and should be avoided in future probe development. Presumably, mutual repulsions of the more highly charged dye molecules lowers the total amount of probe that can bind to the membrane. It may prove possible to increase the sensitivity of impermeant oxonols by exchanging the arylsulfonate groups with highly polar neutral residues. This would reduce the net charge on the probe to -1 and would still provide a membrane-impermeant anchor for the dye.

We are grateful to Amiram Grinvald and Lawrence Cohen for their valuable help with this manuscript. This work was supported by NS 19353 to ASW and by GM 28839 to JCF.

References

Andersen, O.S., Feldberg, S., Nakadomari, H., Levy, S., McLaughlin, S. 1978. Electrostatic interactions among hydrophobic ions in lipid bilayer membranes. *Biophys. J.* **21**:35–70

Bashford, C.L., Chance, B., Smith, J.C., Yoshida, T. 1979. The behavior of oxonol dyes in phospholipid dispersions. *Biophys. J.* **25**:63–80

Cohen, L.B., Salzberg, B.M., Davila, H.V., Ross, W.N., Landowne, D., Waggoner, A.S., Wang, C.H. 1974. Changes in axon fluorescence during activity: Molecular probes of membrane potential. *J. Membrane Biol.* **19**:1–36

Davies, J.T. 1958. Adsorption of long-chain ions. I. *Proc. R. Soc. London A* **245**:417–433

Diamond, J.M., Katz, Y. 1974. Interpretation of nonelectrolyte partition coefficients between dimyristoyl lecithin and water. *J. Membrane Biol.* **17**:121–154

Dragsten, P.R., Webb, W.W. 1978. Mechanism of potential sensitivity of the membrane potential sensitive probe merocyanine 540. *Biochemistry* **17**:5228–5240

Flewelling, R.F., Hubbell, W.L. 1986*a*. Hydrophobic ion interactions with membranes. Thermodynamic analysis of tetraphenylphosphonium binding to vesicles. *Biophys. J.* **49**:531–540

Flewelling, R.F., Hubbell, W.L. 1986*b*. The membrane dipole potential in a total membrane potential model. Applications to hydrophobic ion interactions with membranes. *Biophys. J.* **49**:541–552

George, E.B., Nyirjesy, P., Basson, M., Pratap, P.R., Freedman, J.C., Ernst, L.A., Waggoner, A.S. 1988*a*. Impermeant potential-sensitive oxonol dyes. I. Evidence for an "on-off" mechanism. *J. Membrane Biol.*, **103**:245–253

George, E.B., Nyirjesy, P., Pratap, P.R., Freedman, J.C., Waggoner, A.S. 1988*b*. Impermeant potential-sensitive oxonol dyes: III. The dependence of the absorption signal on membrane potential. *J. Membrane Biol.* **105**:55–64

Gupta, R.K., Salzberg, B.M., Grinvald, A., Cohen, L.B., Kamino, K., Lesher, S., Boyle, M.B., Waggoner, A.S., Wang, C.H. 1981. Improvements in optical methods for measuring rapid change in membrane potential. *J. Membrane Biol.* **58**:123–137

Honig, B.H., Hubbell, W.L., Flewelling, R.F. 1986. Electrostatic interactions in membranes and proteins. *Annu. Rev. Biophys. Bioeng.* **15**:163–193

Ketterer, B., Neumcke, B., Läuger, P. 1972. Transport mechanism of hydrophobic ions through lipid bilayer membranes. *J. Membrane Biol.* **5**:225–245

Krasne, S. 1980. Interactions of voltage-sensing dyes with membranes. II. Spectrophotometric and electrical correlates of cyanine dye adsorption to membranes. *Biophys. J.* **30**:441–462

McLaughlin, S. 1977. Electrostatic potentials at solution-membrane interfaces. *Curr. Top. Membr. Transp.* **9**:71–94

Sims, P.J., Waggoner, A.S., Wang, C.H. Hoffman, J.F. 1974. Studies on the mechanism by which cyanine dyes measure membrane potential in red blood cells and phosphatidylcholine vesicles. *Biochemistry* **13**:3315–3323

Smith, J.C., Frank, S.J., Bashford, C.L., Chance, B., Rudkin, B. 1980. Kinetics of the association of potential-sensitive dyes with model and energy-transducing membranes: Implications for fast probe response times. *J. Membrane Biol.* **54**:127–139

Tanford, C. 1980. The Hydrophobic Effect. (2nd ed.) Wiley-Interscience, New York

Waggoner, A.S. 1976. Optical probes of membrane potential. *J. Membrane Biol.* **27**:317–334

Waggoner, A.S., Grinvald, A. 1977. Mechanism of rapid optical changes of potential sensitive dyes. *Ann. N.Y. Acad. Sci.* **303**:217–241

Waggoner, A.S., Wang, C.H., Tolles, R.L. 1977. Mechanism of potential-dependent light absorption changes of lipid bilayer membranes in the presence of cyanine and oxonol dyes. *J. Membrane Biol.* **33**:109–140

Wolf, B.E., Waggoner, A.S. 1986. Optical studies of the mechanism of membrane potential sensitivity of merocyanine 540. *In:* Optical Methods in Cell Physiology. P. DeWeer, and B.M. Salzberg, editors. pp. 101–113. John Wiley and Sons, New York

Received 5 January 1988; revised 2 May 1988